ACS Energy LETTERS

http://pubs.acs.org/journal/aelccp

Redox-Active Polymers Designed for the Circular Economy of Energy Storage Devices

Siew Ting Melissa Tan, Tyler J. Quill, Maximilian Moser, Garrett LeCroy, Xingxing Chen, Yilei Wu, Christopher J. Takacs, Alberto Salleo, and Alexander Giovannitti*

Cite This: *ACS Energy Lett.* 2021, 6, 3450−3457

Read Online

ACCESS | Metrics & More | Article Recommendations | Supporting Information

ABSTRACT: **Electrochemical energy storage is a keystone to support the rapid transition to a low-carbon-emission future for grid storage and transportation. While research on electrochemical energy storage devices has mostly dealt with performance improvements (energy density and power density), little attention has been paid to designing devices that can be recycled with low cost and low environmental impact. Thus, next-generation energy storage devices should also address the integration of recyclability into the device design. Here, we demonstrate recyclable energy storage devices based on solution-processable redox-active conjugated polymers. The high electronic and ionic charge transport in these polymers enables the operation of single-phase electrodes in aqueous electrolytes with C-rates >100 with good electrochemical stability when the cell is charged to 1.2 V. Finally, we demonstrate the recyclability of these devices, achieving >85% capacity retention in each recycling step. Our work provides a framework for developing recyclable devices for sustainable energy storage technologies.**

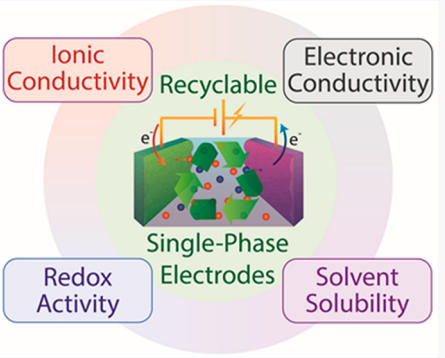

The global move toward decarbonization will result in a tremendous growth of the energy storage industry, spurred by the transition toward intermittent renewable energy sources[1] and the electric-vehicle revolution.[2,3] The state of the art energy storage device is the Li-ion battery (LIB), and its exceptional performance has enabled its ubiquity in high-energy-density applications in consumer electronics,[4] electric vehicles,[3] and grid storage.[5] Current limitations of LIB lifetimes arise from the mechanical failure of electrodes due to volumetric expansion/contraction,[6] solid electrolyte interface formation,[7] Li dendrite formation,[8] and oxygen evolution.[9] While some LIBs may be repurposed for a second life, such as the translation of spent EV batteries to the grid and residential services,[10] these approaches do not address the need for upcycling of their constituent materials, resulting in the majority of these devices ultimately ending up in landfills at their end of life (EOL).

Present battery research has prioritized high performance (high capacity, stability, and low self-discharge) by identifying and ameliorating the aforementioned sources of degradation via judicious materials and electrochemical design. However, recyclability is not integrated into the design of these devices and is mostly treated as an afterthought.[11] Encouraging greater industry adoption of recycling processes requires achieving higher recycling efficiencies and utilizing simpler and lower-energy processes. One potential approach to ease the recycling of energy storage devices is using liquid extraction processes to separate individual components of the device,[12] driven by the concept of the selective extraction of materials in orthogonal solvents. To achieve simple and effective extraction of the cathode and anode materials, the redox-active materials should ideally function as single-phase electrode materials,[11] thereby avoiding additional separation steps of additives and binders during the recycling process. Furthermore, the materials should achieve high solubility in the solvents used for recycling, while being insoluble in the operating electrolyte.

One class of materials compatible with the proposed approach is redox-active conjugated polymers.[13] Recent progress in their design has enabled the development of solution-processable redox-active polymers with balanced electronic/ionic transport properties.[14−19] The functionalization of conjugated polymers with ion-transporting side chains has resulted in new applications as cathode and anode materials in energy storage devices operating in organic[20] or aqueous electrolytes.[14,21−25] Additionally, the design of polymer side chains enables solubility in organic solvents, allowing for ease in solution processing during device fabrication.[14,17] Recent work following this approach showed that single-phase electrodes achieved high

Received: August 3, 2021

Downloaded via STANFORD UNIV on September 10, 2021 at 02:04:05 (UTC).
See https://pubs.acs.org/sharingguidelines for options on how to legitimately share published articles.

© XXXX American Chemical Society

https://doi.org/10.1021/acsenergylett.1c01625
ACS Energy Lett. 2021, 6, 3450−3457

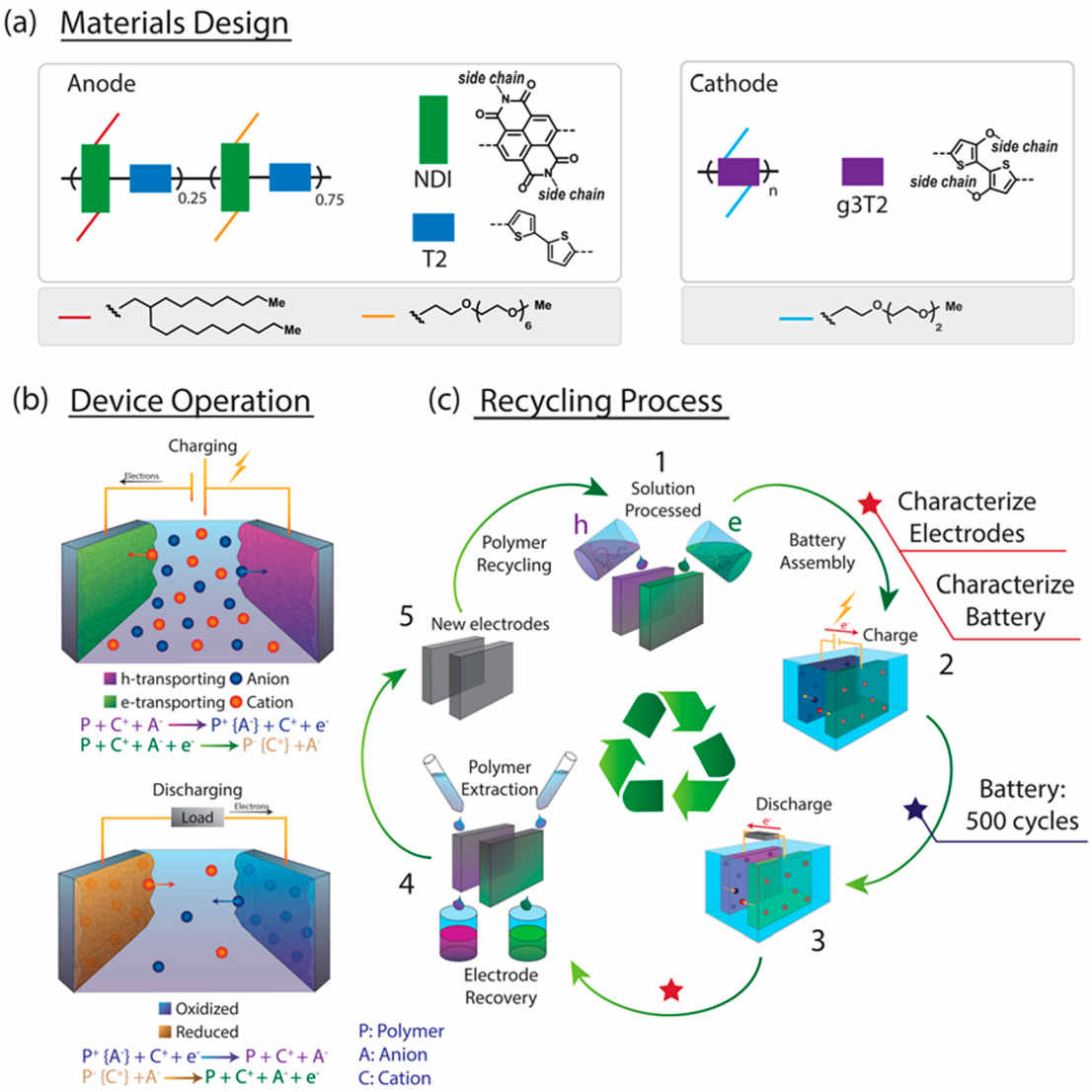

Figure 1. Operating mechanism of polymeric energy storage devices and illustration of the recycling concept. (a) Schematic of the chemical structures of the electron-transporting conjugated copolymer P-75 used as the anode and the hole-transporting conjugated homopolymer p(g3T2) used as the cathode. Backbone: green rectangles represent NDI units, blue rectangles the bithiophene units (T2), and purple rectangles the g3T2 units. Side chains: alkyl chains are shown in red and glycol chains in orange or blue. (b) Charging and discharging mechanism of polymer electrodes in an aqueous electrolyte. During charging: oxidation of the cathode and injection of hydrated anions into the film, as well as reduction of the anode and injection of hydrated cations into the film. During discharging: the oxidized hole-transporting polymer is reduced to its neutral state, resulting in the ejection of anions from the oxidized cathode. The reduced electron-transporting polymer is oxidized to its neutral state, resulting in the removal of cations from the reduced anode. (c) Recycling procedure of electrochemical cells; (1) Polymer deposition; (2) electrochemical characterization of individual electrodes; (3) cell assembly in aqueous electrolyte followed by characterization of the electrochemical properties; (4) extraction of the redox-active polymers; (5) redeposition of polymer solutions on new current collector substrates. Red stars indicate stages where electrodes and the battery are characterized.

charge capacity retention, even at C-rates >1000.[14] While there remains room for improvement to achieve high specific capacities of redox-active conjugated polymers, there have already been several structures reported promising theoretical gravimetric capacities exceeding 200 mAh/g.[26]

We report the development of a recyclable energy storage device based on redox-active conjugated polymers that function as additive- and binder-free electrodes on carbon paper substrates in aqueous electrolytes. When they are operated in electrochemical cells, the polymer electrodes achieve stable operation over 1500 charge−discharge cycles with a mass loading >1 mg/cm^2. Judicious polymer design enables high solubility in processing solvents while low solubility is maintained in the operational electrolyte. This allows both cathode and anode electrodes to be extracted by solvent extraction processes with recycling efficiencies of >85% over multiple recycling steps. Our work showcases new directions to address the current shortcomings of materials design with the ultimate goal of simplifying the creation of a circular economy of energy storage devices.

The electrode materials are redox-active polymeric organic semiconductors (Figure 1a), where the anode comprises an electron-transporting and the cathode a hole-transporting conjugated polymer. The anode is a conjugated polymer based on naphthalenetetracarboxylic diimide (NDI) and bithiophene (T2) units,[15] while the cathode material is a conjugated

https://doi.org/10.1021/acsenergylett.1c01625
ACS Energy Lett. 2021, 6, 3450−3457

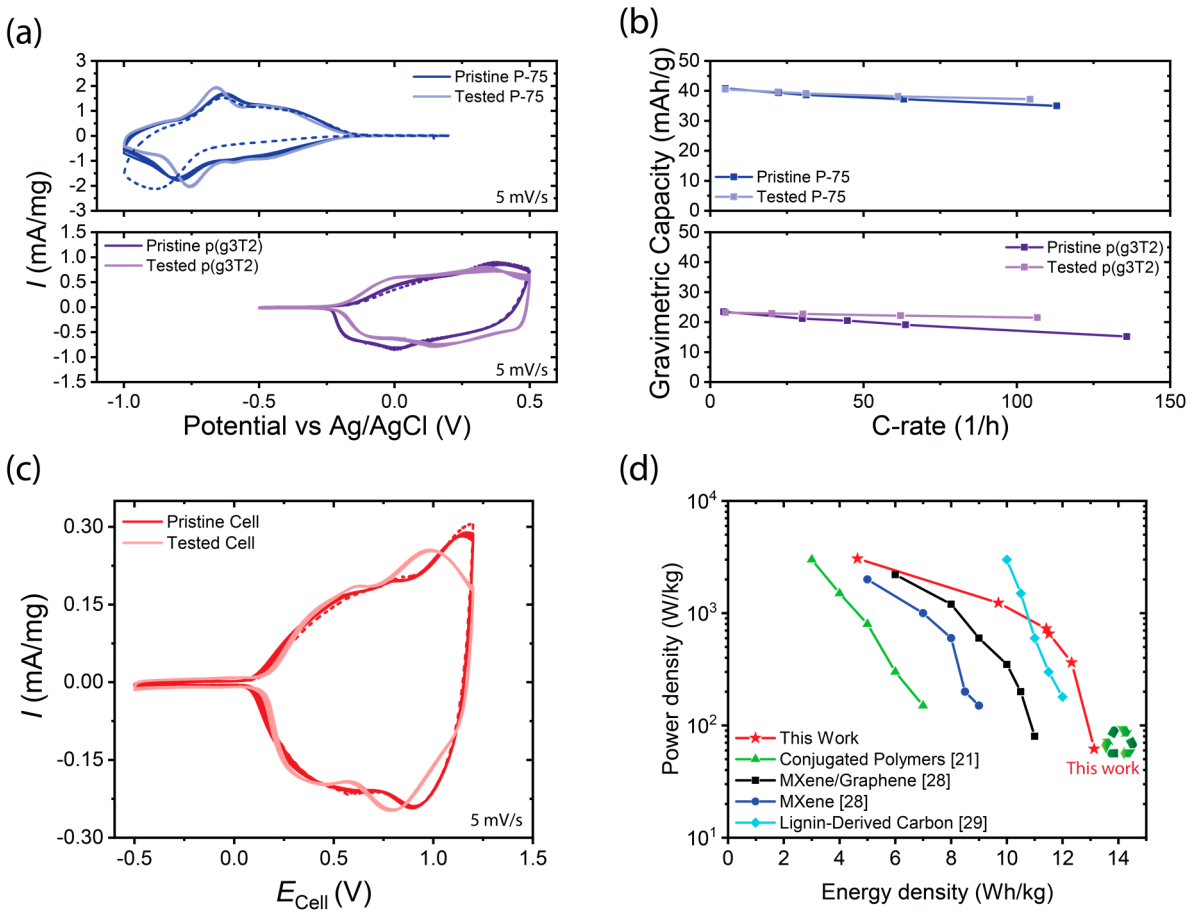

Figure 2. Performance of the energy storage device in aqueous electrolyte. (a) Three-electrode CV measurements of individual polymer electrodes (half cells) at 5 mV/s in 0.1 M NaCl aqueous electrolyte at a low oxygen concentration of the pristine electrode material (dark traces) and after cycling the polymer for 500 charge−discharge cycles (light traces). Dashed lines indicate the first CV cycle of the pristine polymer electrode. The upper panel shows the CV of P-75 (1.0 mg) from +0.2 to −1.0 V vs Ag/AgCl, and the lower panel shows the CV of p(g3T2) (2.0 mg) from −0.5 to +0.5 V vs Ag/AgCl. (b) Three-electrode measurements: gravimetric capacity measurements of the individual electrodes (half cells) at different charging rates in their initial states (pristine electrode, dark traces) and after 500 charge−discharge cycles of the electrochemical cell (tested electrode, light traces). (c) Two-electrode measurements: CV measurements of the assembled cell (full cell) between −0.5 and +1.2 V at 5 mV/s in 0.1 M NaCl aqueous electrolyte at low oxygen concentration showing the performance of the pristine device (pristine device, dark traces) and after conducting 500 charging−discharging cycles (tested device, light trace). The current is normalized by the mass of both polymers. (d) Ragone plot comparing the power and energy density of the full cell with those of other supercapacitor or aqueous electrolyte based energy storage cells.[21,28,29] Note: calculations of the power and energy densities of all presented devices consider only the mass loading of the redox-active materials.

homopolymer based on a dialkoxybithiophene (g3T2) repeat unit.[14] Hydrophilic side chains based on ethylene glycol are attached to the polymer backbone to enable rapid ion transport from the electrolyte into the bulk of the electrode. Furthermore, these side chains are selected to achieve high solubility in organic solvents for processing the electrode materials from solution and enabling subsequent recycling via solvent extraction. Mixed hydrophilic and hydrophobic side chains are attached to the polymer backbone of the anode to control the swelling of the polymer with water molecules from the electrolyte, while simultaneously ensuring that the neutral and charged polymers are insoluble in the aqueous electrolyte.[27] Employing mixed hydrophilic/hydrophobic side chains on the NDI unit has been reported to improve the electrochemical stability of redox-active polymers with long hydrophilic side chains during charging to achieve charge densities beyond one electron per repeat unit.[14,27] Thus, the anode material comprises 25% hydrophobic (branched alkyl side chains ($-CH_2CH(C_8H_{17}C_{10}H_{21})$) and 75% hydrophilic (heptakis(ethylene glycol) ($-CH_2CH_2O)_7Me$)) side chains, referred to as p([75:25]NDI-T2) or P-75, to achieve high solubility in organic solvents.[15] The cathode material (p(g3T2))[14] contains short hydrophilic (triethylene glycol, ($-CH_2CH_2O)_3Me$)) side chains which lead to high electrochemical stability without the need to substitute hydrophilic side chains with hydrophobic side chains. The polymer electrodes p(g3T2) and P-75 are water-insoluble in their neutral and charged states.

During electrochemical charging, holes or electrons (in p(g3T2) or P-75, respectively) are accumulated on the individual polymer backbones. Concurrently, hydrated anions and cations (chloride (Cl^-) and sodium ions (Na^+)) intercalate from the aqueous electrolyte into the bulk of the polymer to electrostatically compensate the electronic charge carriers on the polymer backbones, as illustrated in Figure 1b. The process is reversed during discharge, where the stored energy is released to operate a device. Figure 1c shows a schematic of the recycling process of the energy storage device, starting with the deposition of polymers on fresh electrodes, followed by cell operation and

https://doi.org/10.1021/acsenergylett.1c01625
ACS Energy Lett. 2021, 6, 3450−3457

the recycling procedure (see Methods in the Supporting Information).

Polymer electrodes are prepared by drop-casting polymer solutions from low-boiling-point solvents onto conductive paper substrates to achieve mass loadings of 1.0 and 2.0 mg/cm^2 for P-75 and p(g3T2), respectively. The paper substrates act as the current collectors, and their porous nature supports the volumetric charging of the additive- and binder-free electrodes. We first study the electrochemical properties of individual polymer electrodes using cyclic voltammetry (CV) (Figure 2a) (CVs of the conductive paper substrate as controls are shown in Figure S3 in the Supporting Information). The electron-transporting polymer (P-75) becomes charged between −0.2 and −1.0 V vs Ag/AgCl, showing a redox peak at around −0.7 V vs Ag/AgCl. The first charging cycle (dashed line) occurs at a more negative apparent potential in comparison to the subsequent scans, mostly due to the uptake of water molecules (swelling) during the first charging cycle that subsequently improves the ion-transporting properties of the polymer. The hole-transporting polymer (p(g3T2)) becomes charged between −0.2 and +0.5 V vs Ag/AgCl, for which a shift to a more negative apparent potential is also observed over incremental charge−discharge cycles due to the swelling of the electrode material during operation.[18]

To evaluate the gravimetric capacity and the charging rates of the single-phase polymer electrodes, galvanostatic (chronopotentiometry (CP)) measurements were conducted. Figure 2b summarizes the results of the gravimetric capacity of the individual electrodes vs C-rate in 0.1 M NaCl aqueous electrolyte. At a C-rate of 5, p(g3T2) and P-75 have gravimetric capacities of 23 and 40 mAh/g, respectively. The higher gravimetric capacity of P-75 stems from the donor−acceptor type nature of the polymer, where it has been reported that the NDI unit can stabilize up to two electrons per repeat unit, resulting in the formation of the bipolaronic state.[14,30] In comparison, for p(g3T2), the injected holes are distributed (delocalized) along the polymer backbone, resulting in lower charge carrier densities per repeat unit (estimated to be up to two holes per three repeat units[14]). A higher degree of charging may be achieved for p(g3T2); however, this comes at the cost of lower electrochemical stability due to chemical side reactions between the oxidized polymer and solvent molecules and ions of the electrolyte.[14] Encouragingly, P-75 achieves 78% of its theoretical gravimetric capacity (50.9 mAh/g, considering two electrons per repeat unit) and p(g3T2) achieves 84% of its theoretical gravimetric capacity (27.4 mAh/g, considering 0.5 holes per repeat unit). These findings show that high fractions of the redox-active sites are accessible in additive- and binder-free polymer electrodes. Despite the variation in the C-rates from 5 to 100, the electrodes each retain >70% of the specific capacity, as shown in Figure 2b and Figure S4 in the Supporting Information.

We assembled the energy storage device with p(g3T2) (1.0 mg) as the positive electrode (cathode) and P-75 (2.0 mg) as the negative electrode (anode) and achieved cell voltages of up to 1.2 V. Higher cell voltages may be achieved, but at the risk of overcharging the individual electrodes, accelerating device degradation. Finally, we evaluated the electrochemical stability of the individual electrodes (Figure 2a) and the energy storage device (Figure 2c) after 500 galvanostatic charging/discharging cycles. Encouragingly, high electrochemical stability is observed for both individual electrode materials and the energy storage device after 500 charge−discharge cycles. Additionally, the electrode capacities increased after 500 charge−discharge cycles, which is more apparent at high C-rates (Figure 2b). We hypothesize that the repeated charging and discharging of the polymers, which involves shuttling of ions and water molecules into and out of the bulk of the polymer, results in improved ionic transport properties of the polymer electrodes and thus enables the utilization of a higher fraction of the redox-active sites in the bulk of the material.

The Ragone plot in Figure 2d benchmarks the performance of the energy storage device with other electrochemical energy storage devices reported in the literature (accounting for only the weight of the redox-active materials).[21,28,29] The device achieves an energy density of 4.5 Wh/kg at a power density of 3000 W/kg. In comparison with its counterparts in the class of aqueous-based electrochemical capacitors, our work demonstrates a higher energy density in comparison to the average reported values in the literature.[14,21,31] To our knowledge, the only other class of batteries intentionally designed to be recyclable is lead-acid batteries.[32] While Pb-acid batteries exhibit around 1 order of magnitude greater energy density in comparison to the developed recyclable polymer energy storage device, the presented polymer device exhibits approximately 2 orders of magnitude greater power density. Furthermore, our device operates at 2 orders of magnitude larger energy densities in comparison to electrolytic capacitors[33] and maintains low self-discharge rates, retaining >91% of its charge after 1 h (Figure S6 in the Supporting Information). This enables applications in low-energy-density applications that require fast charging and discharging such as energy storage from intermittent sources, regenerative braking, as well as operating low-power sensors for lab-on-a-chip or other IoT devices (see powering of an LED in Figure S7 in the Supporting Information).

After establishing a stable aqueous polymer energy storage device, we next analyze the recycling efficiency of the device. Leveraging the advantages of single-phase electrodes, we employ solvent extraction processes to recycle the device reported in Figure 2c twice using an ambient recycling method (Methods and Figure S2 in the Supporting Information). Encouragingly, >85% of the gravimetric capacity of the individual electrodes is retained after each recycling step and there is a remarkable 76% retention of charge capacity after recycling the energy storage device twice and after a total of 1500 charging/discharging cycles (Figure 3a and Figure S8 in the Supporting Information).

Similar to the individual electrodes shown in Figure 2b, the energy storage device retains up to 75% of the specific capacity when the C-rate is increased from 5 to 150, with Coulombic efficiencies of close to 100% (Figure 3b)). Notably, the capacity dependences with respect to C-rate of the pristine and recycled devices are comparable, showing that the recycling process does not harm the electronic and ionic charge transport properties of the redox-active polymers. Figure 3c and Figure S9 in the Supporting Information present the changes in the capacity for the energy storage device as well as for the individual electrodes as a measure to identify which electrode experiences the greatest degradation. We observed that the majority of the capacity loss occurred during the recycling steps (loss of 7% for recycling #1 and 21% for recycling #2), where P-75 experiences the largest drop in capacity (10−20% loss; see Table S1 in the Supporting Information). Further details of each testing stage are provided in Figures S5 and S10−S13 in the Supporting Information.

To further investigate the loss in capacity of the electrodes, we evaluated the chemical stability of the polymers by comparing the chemical compositions of the pristine and recycled polymers

https://doi.org/10.1021/acsenergylett.1c01625
ACS Energy Lett. 2021, 6, 3450−3457

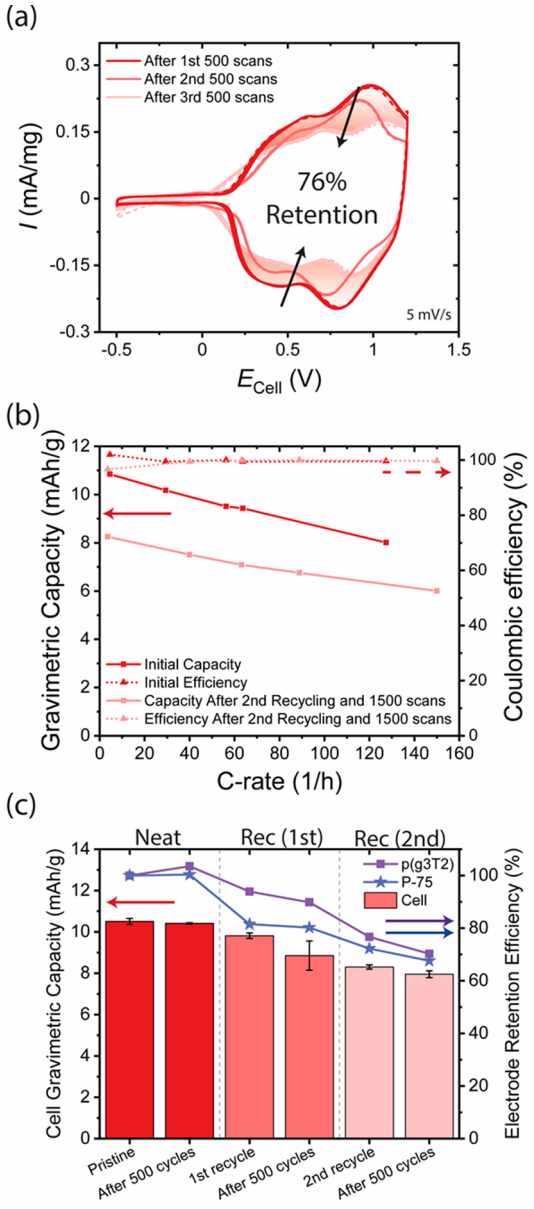

Figure 3. Recycling efficiency of the energy storage device (full cell). (a) CV measurement of the energy storage device between −0.5 and +1.2 V at 5 mV/s after charging/discharging for 500 cycles, after the first recycling of the device and another 500 subsequent charging/discharging cycles, and in its final state after recycling the device for a second time and a total of 1500 charge−discharge cycles. The first scan is shown as a dashed line and the shaded region indicates the total loss in capacity (24%). (b) Gravimetric capacity (solid traces) and Coulombic efficiency (dashed traces) vs C-rate plot of the cell in its initial and final states after recycling the energy storage device twice and a total of 1500 charge−discharge cycles. (c) Changes in the gravimetric capacity of the energy storage device (red columns) and individual electrode (half cell) retention efficiency (traces above columns: purple, cathode; blue, anode) at different stages of testing: pristine device, after the first 500 charge−discharge cycles, after the first recycling, after the second 500 charge−discharge cycles, after the second recycling, and after the third 500 charge−discharge cycles. We note that the trendlines for the individual electrodes (p(g3T2) and P-75) act as guidelines to illustrate the drop in capacity, rather than being actual fits of the curve.

using proton nuclear magnetic resonance (^{1}H NMR) spectroscopy, X-ray photoelectron spectroscopy (XPS), UV−vis spectroscopy, grazing-incidence wide-angle X-ray scattering (GIWAXS), and mass spectrometry (matrix-assisted laser desorption/ionization time of flight (MALDI-TOF)). The results from ^{1}H NMR spectroscopy and XPS measurements show that p(g3T2) and P-75 are chemically and electrochemically stable after multiple charging/discharging cycles and after the recycling of the polymer electrodes (Figures S15−S22). However, we observed residual p(g3T2) on the current collector after solvent extraction (Figure S22), which is a result of oxidation of the polymer under ambient conditions that lowers the solubility of the polymer in organic solvents and thus decreases the extraction yield. By minimizing the exposure of the electrode to molecular oxygen, we improved the recycling efficiency of p(g3T2) from 30% to 85% (Figure S29). Interestingly, a high chemical stability for P-75 is only observed when anhydrous solvents are employed during the recycling step and heating is avoided (anhydrous recycling method; see Methods in the Supporting Information). In contrast, recycling of P-75 with wet (water-containing) organic solvents at elevated temperatures results in chemical modification of the polymer P-75, most likely due to a ring-opening reaction of the imides of the NDI repeat unit (Figures S16, S20a−d, and S26e in the Supporting Information). Encouragingly, both polymers have comparable UV−vis absorption spectra (Figure S23 in the Supporting Information), molecular weight distributions (Figure S24 in the Supporting Information), and GIWAXS diffraction patterns (Figures S25−S28 in the Supporting Information) before and after recycling when the anhydrous recycling method is employed, showing that both polymers are stable under the recycling conditions. Finally, electrodes recycled using the anhydrous recycling method achieve a retention of capacity comparable to that of electrodes recycled under ambient conditions (Figure S14 in the Supporting Information), with the added benefit of avoiding chemical modifications of the anode material P-75.

We developed recyclable redox-active polymer electrodes that function in aqueous-based electrolytes with high electrochemical stability and maintain their specific capacities after several recycling steps. We took advantage of the outstanding electronic and ionic charge transport properties of conjugated polymers functionalized with hydrophilic side chains to employ them as single-phase electrodes. The side chains were chosen to enable device operation in environmentally friendly electrolytes such as salty water. Additionally, they achieve high solubility in organic solvents for ease of processing the redox-active compounds from solution, paving the way for low-cost fabrication of devices as well as efficient extraction of redox-active materials at the EOL. Simpler and more cost efficient extraction processes can be developed for materials that function as additive- and binder-free redox-active materials, in comparison to electrodes with mixed phases. For example, the addition of binders and additives may result in the formation of insoluble particles, resulting in the trapping of redox-active molecules that lowers the recycling efficiency and complicates the recycling of large-scale devices. By designing redox-active materials that function as additive- and binder-free electrodes with high solubility in the processing solvent, we show that high recovery efficiency can be achieved by employing one-step extraction processes. Our approach of integrating recyclability within materials design instead of leaving recycling as an afterthought allows our process to avoid additional separation and purification steps.

https://doi.org/10.1021/acsenergylett.1c01625
ACS Energy Lett. 2021, 6, 3450−3457

In its present state, our device can be utilized for high-power-density and low-energy-density applications that rely on rapid charging and discharging (energy storage from intermittent sources, regenerative braking systems, and start/stop systems). In addition, our developed energy storage device achieves high stability in pH-neutral aqueous electrolytes and enables the potential development of on-body biosensors or lab-on-a-chip devices, where hazardous electrolytes must be avoided. In comparison to other polymeric energy storage devices operated in pH-neutral aqueous electrolytes, our device achieves higher capacities and cell voltages[21] as well as excellent redox stabilities beyond 1500 charge−discharge cycles. We further show that p(g3T2) can be processed and recycled from dimethylformamide (DMF), a more sustainable solvent in comparison to chloroform (Figure S30 in the Supporting Information). Although our recyclable energy storage device targets a different application space due to the lower energy density in comparison to lead-acid batteries, the recycling process of our device is simple and has a low environmental impact, since all components can be recovered and reused, including the solvents used for extraction and processing of the polymers.

The ability to control the redox activity and electronic conductivity (via backbone design) as well as the ionic conductivity and solubility (via side chain engineering) of conjugated polymers presents a wealth of opportunities in the design of single-phase polymeric electrodes. To extend the utility of these recyclable redox-active polymers to energy storage devices, further work should address improving the energy density of redox-active polymers. One strategy includes functionalizing side chains with redox-active molecules (quinones or hydroquinones[31] or nitroxide radicals based on 2,2,6,6-tetramethylpiperindine-1-oxyl (TEMPO)[34]) while high solubility is maintained to process polymers from solution. Alternatively, polymer backbones can be designed to store more than two electronic charge carriers per repeat unit.[26]

The role of the side chain expands beyond solubilizing the polymer in organic solvents to process the redox-active materials from solution and to enable recycling. We further show that the side chain is important for transporting ions and electrolyte solvent molecules into the bulk of the polymer to utilize high fractions of the theoretical capacity of the polymer. To demonstrate this concept, we evaluated the electrochemical performance of a hole-transporting polymer with shorter hydrophilic side chains (diethylene glycol side chains for p(g2T2), theoretical gravimetric capacity of 33.4 mAh/g)[35] instead of triethylene glycol side chains for p(g3T2) (theoretical gravimetric capacity of 27.4 mAh/g) (Figure S31). Surprisingly, instead of observing an increase of the gravimetric capacity, we observed a lower gravimetric capacity for p(g2T2), demonstrating the importance of the side chain in transporting ions into the bulk of the polymer. Additionally, the lower solubility of p(g2T2) in organic solvents prevented the recycling of the polymer at the EOL of the device.

The adoption of this technology requires further work to achieve economies of scale, including lowering the production cost of the redox-active polymers: for instance, via large-scale flow-chemistry synthesis.[36] Finally, the environmental footprint of device fabrication and the recycling process can be further minimized by designing polymers that can be processed from green solvents[37] and are biodegradable.[38] Further improvements in recycling efficiencies through utilizing large-scale batch processes will pave the way for a circular economy of energy storage devices based on solution-processable redox-active polymers.

■ ASSOCIATED CONTENT

Supporting Information

The Supporting Information is available free of charge at https://pubs.acs.org/doi/10.1021/acsenergylett.1c01625.

Experimental procedure for fabrication and recycling, electrochemical measurements of individual polymer electrodes and cells, chemical characterization of the polymers before and after testing and recycling (^{1}H NMR spectroscopy, XPS measurements, UV−vis spectroscopy, determination of the molecular weight by MALDI-ToF mass spectrometry, and GIWAXS measurements), EIS measurements, and battery checklist (PDF)

■ AUTHOR INFORMATION

Corresponding Author

Alexander Giovannitti − *Department of Materials Science and Engineering, Stanford University, Stanford, California 94305, United States;* orcid.org/0000-0003-4778-3615; Email: ag19@stanford.edu

Authors

Siew Ting Melissa Tan − *Department of Materials Science and Engineering, Stanford University, Stanford, California 94305, United States;* orcid.org/0000-0003-3343-9223

Tyler J. Quill − *Department of Materials Science and Engineering, Stanford University, Stanford, California 94305, United States;* orcid.org/0000-0003-2906-0747

Maximilian Moser − *Department of Chemistry, Chemistry Research Laboratory, University of Oxford, Oxford OX1 3TA, U.K.;* orcid.org/0000-0002-3293-9309

Garrett LeCroy − *Department of Materials Science and Engineering, Stanford University, Stanford, California 94305, United States*

Xingxing Chen − *Physical Science and Engineering Division, King Abdullah University of Science and Technology, Thuwal 23955-6900, Saudi Arabia*

Yilei Wu − *Department of Chemical Engineering, Stanford University, Stanford, California 94305, United States;* orcid.org/0000-0001-6756-1855

Christopher J. Takacs − *Stanford Synchrotron Radiation Lightsource, SLAC National Accelerator Laboratory, Menlo Park, California 94025, United States*

Alberto Salleo − *Department of Materials Science and Engineering, Stanford University, Stanford, California 94305, United States*

Complete contact information is available at: https://pubs.acs.org/10.1021/acsenergylett.1c01625

Notes

The authors declare no competing financial interest.

■ ACKNOWLEDGMENTS

A.G. and A.S. acknowledge funding from the TomKat Center for Sustainable Energy at Stanford University and the StorageX initiative. A.S. and S.T.M.T. gratefully acknowledge support from the National Science Foundation Award CBET #1804915. T.J.Q. and G.L. acknowledge support from the NSF Graduate Research Fellowship Program under grant DGE-1656518. Part of this work was performed at the Stanford Nanofabrication

Facilities (SNF) and Stanford Nano Shared Facilities (SNSF), supported by the National Science Foundation as part of the National Nanotechnology Coordinated Infrastructure under award ECCS-1542152. The authors acknowledge financial support from KAUST, including the Office of Sponsored Research (OSR) award nos. OSR-2018-CRG/CCF-3079, OSR-2019-CRG8-4086, and OSR-2018-CRG7-3749. The authors acknowledge funding from an ERC Synergy Grant SC2 (610115). Use of the Stanford Synchrotron Radiation Lightsource, SLAC National Accelerator Laboratory, is supported by the U.S. Department of Energy, Office of Science, Office of Basic Energy Sciences, under Contract No. DE-AC02-76SF00515.

REFERENCES

(1) Diouf, B.; Pode, R. Potential of Lithium-Ion Batteries in Renewable Energy. *Renewable Energy* **2015**, *76*, 375−380.
(2) Ciez, R. E.; Whitacre, J. F. Examining Different Recycling Processes for Lithium-Ion Batteries. *Nat. Sustain.* **2019**, *2* (2), 148−156.
(3) Nykvist, B.; Nilsson, M. Rapidly Falling Costs of Battery Packs for Electric Vehicles. *Nat. Clim. Change* **2015**, *5* (4), 329−332.
(4) Huang, B.; Pan, Z.; Su, X.; An, L. Recycling of Lithium-Ion Batteries: Recent Advances and Perspectives. *J. Power Sources* **2018**, *399* (June), 274−286.
(5) Dogger, J. D.; Roossien, B.; Nieuwenhout, F. D. J. Characterization of Li-Ion Batteries for Intelligent Management of Distributed Grid-Connected Storage. *IEEE Trans. Energy Convers.* **2011**, *26* (1), 256−263.
(6) Hu, Y.; Zhao, X.; Suo, Z. Averting Cracks Caused by Insertion Reaction In Lithium-Ion Batteries. *J. Mater. Res.* **2010**, *25* (6), 1007−1010.
(7) An, S. J.; Li, J.; Daniel, C.; Mohanty, D.; Nagpure, S.; Wood, D. L. The State of Understanding of the Lithium-Ion-Battery Graphite Solid Electrolyte Interphase (SEI) and Its Relationship to Formation Cycling. *Carbon* **2016**, *105*, 52−76.
(8) Ren, Y.; Shen, Y.; Lin, Y.; Nan, C. W. Direct Observation of Lithium Dendrites inside Garnet-Type Lithium-Ion Solid Electrolyte. *Electrochem. Commun.* **2015**, *57*, 27−30.
(9) Jung, R.; Metzger, M.; Maglia, F.; Stinner, C.; Gasteiger, H. A. Oxygen Release and Its Effect on the Cycling Stability of LiNi x Mn y Co z O 2 (NMC) Cathode Materials for Li-Ion Batteries. *J. Electrochem. Soc.* **2017**, *164* (7), A1361−A1377.
(10) Canals Casals, L.; Amante García, B.; Cremades, L. V. Electric Vehicle Battery Reuse: Preparing for a Second Life. *J. Ind. Eng. Manag.* **2017**, *10* (2), 266−285.
(11) Tan, D. H. S.; Xu, P.; Chen, Z. Enabling Sustainable Critical Materials for Battery Storage through Efficient Recycling and Improved Design: A Perspective. *MRS Energy Sustain* **2020**, *7* (1), 1−13.
(12) Tran, M. K.; Rodrigues, M. T. F.; Kato, K.; Babu, G.; Ajayan, P. M. Deep Eutectic Solvents for Cathode Recycling of Li-Ion Batteries. *Nat. Energy* **2019**, *4* (4), 339−345.
(13) Paulsen, B. D.; Tybrandt, K.; Stavrinidou, E.; Rivnay, J. Organic Mixed Ionic−Electronic Conductors. *Nat. Mater.* **2020**, *19* (1), 13−26.
(14) Moia, D.; Giovannitti, A.; Szumska, A. A.; Maria, I. P.; Rezasoltani, E.; Sachs, M.; Schnurr, M.; Barnes, P. R. F.; McCulloch, I.; Nelson, J. Design and Evaluation of Conjugated Polymers with Polar Side Chains as Electrode Materials for Electrochemical Energy Storage in Aqueous Electrolytes. *Energy Environ. Sci.* **2019**, *12*, 1349−1357.
(15) Giovannitti, A.; Maria, I. P.; Hanifi, D.; Donahue, M. J.; Bryant, D.; Barth, K. J.; Makdah, B. E.; Savva, A.; Moia, D.; Zetek, M.; Barnes, P. R. F.; Reid, O. G.; Inal, S.; Rumbles, G.; Malliaras, G. G.; Nelson, J.; Rivnay, J.; McCulloch, I. The Role of the Side Chain on the Performance of N-Type Conjugated Polymers in Aqueous Electrolytes. *Chem. Mater.* **2018**, *30* (9), 2945−2953.
(16) Moser, M.; Savagian, L. R.; Savva, A.; Matta, M.; Ponder, J. F.; Hidalgo, T. C.; Ohayon, D.; Hallani, R.; Reisjalali, M.; Troisi, A.; Wadsworth, A.; Reynolds, J. R.; Inal, S.; McCulloch, I. Ethylene Glycol-Based Side Chain Length Engineering in Polythiophenes and Its Impact on Organic Electrochemical Transistor Performance. *Chem. Mater.* **2020**, *32* (15), 6618−6628.
(17) Mei, J.; Bao, Z. Side Chain Engineering in Solution-Processable Conjugated Polymers. *Chem. Mater.* **2014**, *26* (1), 604−615.
(18) Gladisch, J.; Stavrinidou, E.; Ghosh, S.; Giovannitti, A.; Moser, M.; Zozoulenko, I.; McCulloch, I.; Berggren, M. Reversible Electronic Solid−Gel Switching of a Conjugated Polymer. *Adv. Sci.* **2020**, *7* (2), 1901144.
(19) Tan, S. T. M.; Giovannitti, A.; Melianas, A.; Moser, M.; Cotts, B. L.; Singh, D.; McCulloch, I.; Salleo, A. High-Gain Chemically Gated Organic Electrochemical Transistor. *Adv. Funct. Mater.* **2021**, *31*, 2010868.
(20) Li, X.; Li, Y.; Sarang, K.; Lutkenhaus, J.; Verduzco, R. Side-Chain Engineering for High-Performance Conjugated Polymer Batteries. *Adv. Funct. Mater.* **2021**, *31*, 2009263.
(21) Volkov, A. V.; Sun, H.; Kroon, R.; Ruoko, T. P.; Che, C.; Edberg, J.; Müller, C.; Fabiano, S.; Crispin, X. Asymmetric Aqueous Supercapacitor Based on P- And n-Type Conducting Polymers. *ACS Appl. Energy Mater.* **2019**, *2* (8), 5350−5355.
(22) Samuel, J. J.; Karrothu, V. K.; Canjeevaram Balasubramanyam, R. K.; Mohapatra, A. A.; Gangadharappa, C.; Kankanallu, V. R.; Patil, S.; Aetukuri, N. P. B. Ionic Charge Storage in Diketopyrrolopyrrole-Based Redox-Active Conjugated Polymers. *J. Phys. Chem. C* **2021**, *125* (8), 4449−4457.
(23) Li, Y.; Liu, L.; Liu, C.; Lu, Y.; Shi, R.; Li, F.; Chen, J. Rechargeable Aqueous Polymer-Air Batteries Based on Polyanthraquinone Anode. *Chem.* **2019**, *5* (8), 2159−2170.
(24) Patil, N.; Mavrandonakis, A.; Jérôme, C.; Detrembleur, C.; Casado, N.; Mecerreyes, D.; Palma, J.; Marcilla, R. High-Performance All-Organic Aqueous Batteries Based on a Poly(Imide) Anode and Poly(Catechol) Cathode. *J. Mater. Chem. A* **2021**, *9* (1), 505−514.
(25) Xu, Y.; Zheng, Y.; Wang, C.; Chen, Q. An All-Organic Aqueous Battery Powered by Adsorbed Quinone. *ACS Appl. Mater. Interfaces* **2019**, *11* (26), 23222−23228.
(26) Liang, Y.; Jing, Y.; Gheytani, S.; Lee, K.-Y.; Liu, P.; Facchetti, A.; Yao, Y. Universal Quinone Electrodes for Long Cycle Life Aqueous Rechargeable Batteries. *Nat. Mater.* **2017**, *16*, 841−848.
(27) Szumska, A. A.; Maria, I. P.; Flagg, L. Q.; Savva, A.; Surgailis, J.; Paulsen, B. D.; Moia, D.; Chen, X.; Griggs, S.; Mefford, J. T.; Rashid, R. B.; Marks, A.; Inal, S.; Ginger, D. S.; Giovannitti, A.; Nelson, J. Reversible Electrochemical Charging of N-Type Conjugated Polymer Electrodes in Aqueous Electrolytes. *J. Am. Chem. Soc.* **2021**.
(28) Yan, J.; Ren, C. E.; Maleski, K.; Hatter, C. B.; Anasori, B.; Urbankowski, P.; Sarycheva, A.; Gogotsi, Y. Flexible MXene/Graphene Films for Ultrafast Supercapacitors with Outstanding Volumetric Capacitance. *Adv. Funct. Mater.* **2017**, *27* (30), 1701264.
(29) Fu, F.; Yang, D.; Zhang, W.; Wang, H.; Qiu, X. Green Self-Assembly Synthesis of Porous Lignin-Derived Carbon Quasi-Nanosheets for High-Performance Supercapacitors. *Chem. Eng. J.* **2020**, *392*, 123721.
(30) Liang, Y.; Chen, Z.; Jing, Y.; Rong, Y.; Facchetti, A.; Yao, Y. Heavily N-Dopable π-Conjugated Redox Polymers with Ultrafast Energy Storage Capability. *J. Am. Chem. Soc.* **2015**, *137* (15), 4956−4959.
(31) Strietzel, C.; Sterby, M.; Huang, H.; Strømme, M.; Emanuelsson, R.; Sjödin, M. An Aqueous Conducting Redox Polymer Based Proton Battery That Can Withstand Rapid Constant-voltage Charging and Sub-zero Temperatures. *Angew. Chem., Int. Ed.* **2020**, *59*, 9631.
(32) Gies, E. Recycling: Lazarus Batteries. *Nature* **2015**, *526* (7575), S100−S101.
(33) Meng, C.; Maeng, J.; John, S. W. M.; Irazoqui, P. P. Ultrasmall Integrated 3d Micro-Supercapacitors Solve Energy Storage for Miniature Devices. *Adv. Energy Mater.* **2014**, *4* (7), 1301269.
(34) Kunz, T. K.; Wolf, M. O. Electrodeposition and Properties of TEMPO Functionalized Polythiophene Thin Films. *Polym. Chem.* **2011**, *2* (3), 640−644.
(35) Moser, M.; Gladisch, J.; Ghosh, S.; Hidalgo, T. C.; Ponder, J. F.; Sheelamanthula, R.; Thiburce, Q.; Gasparini, N.; Wadsworth, A.; Salleo, A.; Inal, S.; Berggren, M.; Zozoulenko, I.; Stavrinidou, E.;

McCulloch, I. Controlling Electrochemically Induced Volume Changes in Conjugated Polymers by Chemical Design: From Theory to Devices. *Adv. Funct. Mater.* **2021**, *31*, 2100723.
(36) Bannock, J. H.; Krishnadasan, S. H.; Nightingale, A. M.; Yau, C. P.; Khaw, K.; Burkitt, D.; Halls, J. J. M.; Heeney, M.; De Mello, J. C. Continuous Synthesis of Device-Grade Semiconducting Polymers in Droplet-Based Microreactors. *Adv. Funct. Mater.* **2013**, *23* (17), 2123−2129.
(37) Chen, X.; Liu, X.; Burgers, M. A.; Huang, Y.; Bazan, G. C. Green-Solvent-Processed Molecular Solar Cells. *Angew. Chem.* **2014**, *126* (52), 14606−14609.
(38) Uva, A.; Lin, A.; Babi, J.; Tran, H. Bioderived and degradable polymers for transient electronics. *J. Chem. Technol. Biotechnol.* **2021**.

https://doi.org/10.1021/acsenergylett.1c01625
ACS Energy Lett. 2021, 6, 3450−3457